Inhibition of ERK5 Elicits Cellular Senescence in Melanoma via the Cyclin-Dependent Kinase Inhibitor p21

Alessandro Tubita[1], Zoe Lombardi[1], Ignazia Tusa[1], Azzurra Lazzeretti[1], Giovanna Sgrignani[1], Dimitri Papini[1], Alessio Menconi[1], Sinforosa Gagliardi[2], Matteo Lulli[1], Persio Dello Sbarba[1], Azucena Esparís-Ogando[3], Atanasio Pandiella[3,4], Barbara Stecca[2], and Elisabetta Rovida[1]

ABSTRACT

Melanoma is the deadliest skin cancer with a very poor prognosis in advanced stages. Although targeted and immune therapies have improved survival, not all patients benefit from these treatments. The mitogen-activated protein kinase ERK5 supports the growth of melanoma cells *in vitro* and *in vivo*. However, ERK5 inhibition results in cell-cycle arrest rather than appreciable apoptosis. To clarify the role of ERK5 in melanoma growth, we performed transcriptomic analyses following ERK5 knockdown in melanoma cells expressing BRAFV600E and found that cellular senescence was among the most affected processes. In melanoma cells expressing either wild-type or mutant (V600E) BRAF, both genetic and pharmacologic inhibition of ERK5 elicited cellular senescence, as observed by a marked increase in senescence-associated β-galactosidase activity and p21 expression. In addition, depletion of ERK5 from melanoma cells resulted in increased levels of CXCL1, CXCL8, and CCL20, proteins typically involved in the senescence-associated secretory phenotype. Knockdown of p21 suppressed the induction of cellular senescence by ERK5 blockade, pointing to p21 as a key mediator of this process. *In vivo*, ERK5 knockdown or inhibition with XMD8–92 in melanoma xenografts promoted cellular senescence. Based on these results, small-molecule compounds targeting ERK5 constitute a rational series of prosenescence drugs that may be exploited for melanoma treatment.

Significance: This study shows that targeting ERK5 induces p21-mediated cellular senescence in melanoma, identifying a prosenescence effect of ERK5 inhibitors that may be exploited for melanoma treatment.

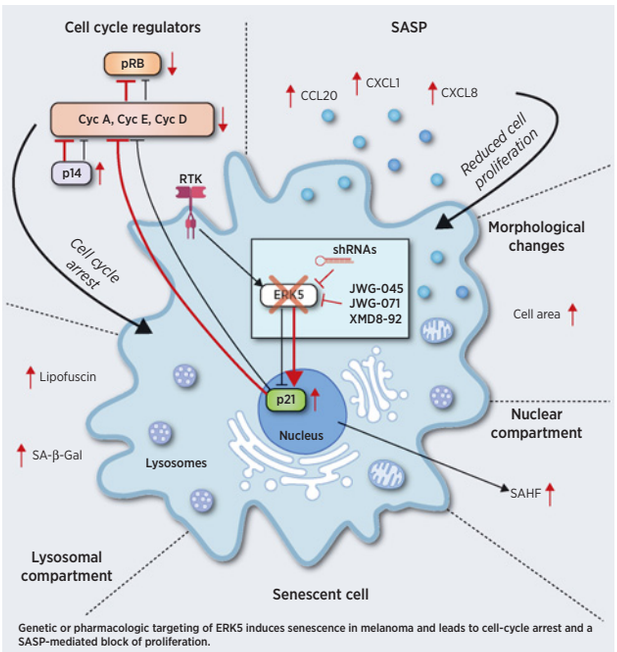

Genetic or pharmacologic targeting of ERK5 induces senescence in melanoma and leads to cell-cycle arrest and a SASP-mediated block of proliferation.

Introduction

Malignant melanoma is one of the most aggressive cancer and its incidence is increasing worldwide. Early-stage disease can be cured in the majority of cases, while late-stage melanoma is a highly lethal disease (1). Genomic sequencing studies of melanomas have found mutations in BRAF, NRAS, and NF1 that hyperactivate the mitogen-activated protein kinases (MAPK) extracellular signal-regulated kinase 1 and 2 (ERK1/2), thus supporting cell proliferation (2, 3). These findings allowed the development of BRAF- and MEK1/2-targeting drugs that, together with immunotherapy, increased the overall survival of melanoma patients (4). However, either the lack of responsiveness to immunotherapy or the presence of intrinsic and acquired resistance to BRAF-MEK1/2 inhibitors limit the benefits of available therapies (5, 6).

ERK5 is involved in cell survival, antiapoptotic signaling, proliferation and differentiation of several cell types, as well as angiogenesis (7), and plays a relevant role in the biology of cancer (8). ERK5 activation is achieved through MEK5-dependent phosphorylation, that stimulates ERK5 nuclear translocation, a key event for cell proliferation (9, 10).

Cellular senescence, a permanent state of cell-cycle arrest, is widely recognized as a potent tumor-suppressive mechanism (11, 12),

[1]Department of Experimental and Clinical Biomedical Sciences "Mario Serio", University of Florence, Florence, Italy. [2]Core Research Laboratory - Institute for Cancer Research and Prevention (ISPRO), Florence, Italy. [3]Instituto de Biología Molecular y Celular del Cáncer (IBMCC-CIC), Instituto de Investigación Biomédica de Salamanca (IBSAL), CIBERONC, Salamanca, Spain. [4]CSIC, Salamanca, Spain.

Note: Supplementary data for this article are available at Cancer Research Online (http://cancerres.aacrjournals.org/).

A. Tubita, Z. Lombardi, and I. Tusa equally contributed to the article.

Corresponding Author: Elisabetta Rovida, Department of Experimental and Clinical Biomedical Sciences, Università di Firenze, Viale G.B. Morgagni, 50, Firenze 50134, Italy. Phone: 3905-5275-1320; E-mail: elisabetta.rovida@unifi.it

Cancer Res 2022;82:447–57

doi: 10.1158/0008-5472.CAN-21-0993

so that induction of senescence is included among the possible strategies to fight cancer (12, 13). Melanoma is frequently characterized by the loss of the pathways supporting cellular senescence that would prevent tumor growth and progression (14). We previously showed that ERK5 inhibition reduces the growth of melanoma, determining a block of the cell cycle rather than inducing apoptosis (15). Because MAPK are frequently involved in cellular senescence (16, 17), we investigated the effects of ERK5 targeting on senescence with the aim to identify a novel therapeutic strategy for melanoma.

Materials and Methods

Cells and cell culture

A375 melanoma cells (18) were obtained from ATCC; SK-Mel-5 melanoma cells (19) were kindly provided by Dr. Laura Poliseno (CRL-ISPRO, Pisa, Italy). SSM2c melanoma cells were already described (Supplementary Table S1; ref. 20). Cells were maintained in DMEM supplemented with 10% heat-inactivated fetal bovine serum (FBS), 2 mmol/L glutamine, 50 U/mL penicillin, and 50 mg/mL streptomycin (EuroClone). Cell lines were yearly authenticated by cell profiling (Promega PowerPlex Fusion System Kit; BMR Genomics s.r.l). Presence of *Mycoplasma* was periodically tested by PCR.

Drugs

ERK5 inhibitor XMD8–92 (21) and MEK5 inhibitor BIX02189 (22) were from MedChemExpress LLC.

Cell lysis and Western blotting

Total cell lysates and nuclear–cytoplasmic fractions were obtained using Laemmli buffer or hypotonic buffer, respectively, as reported

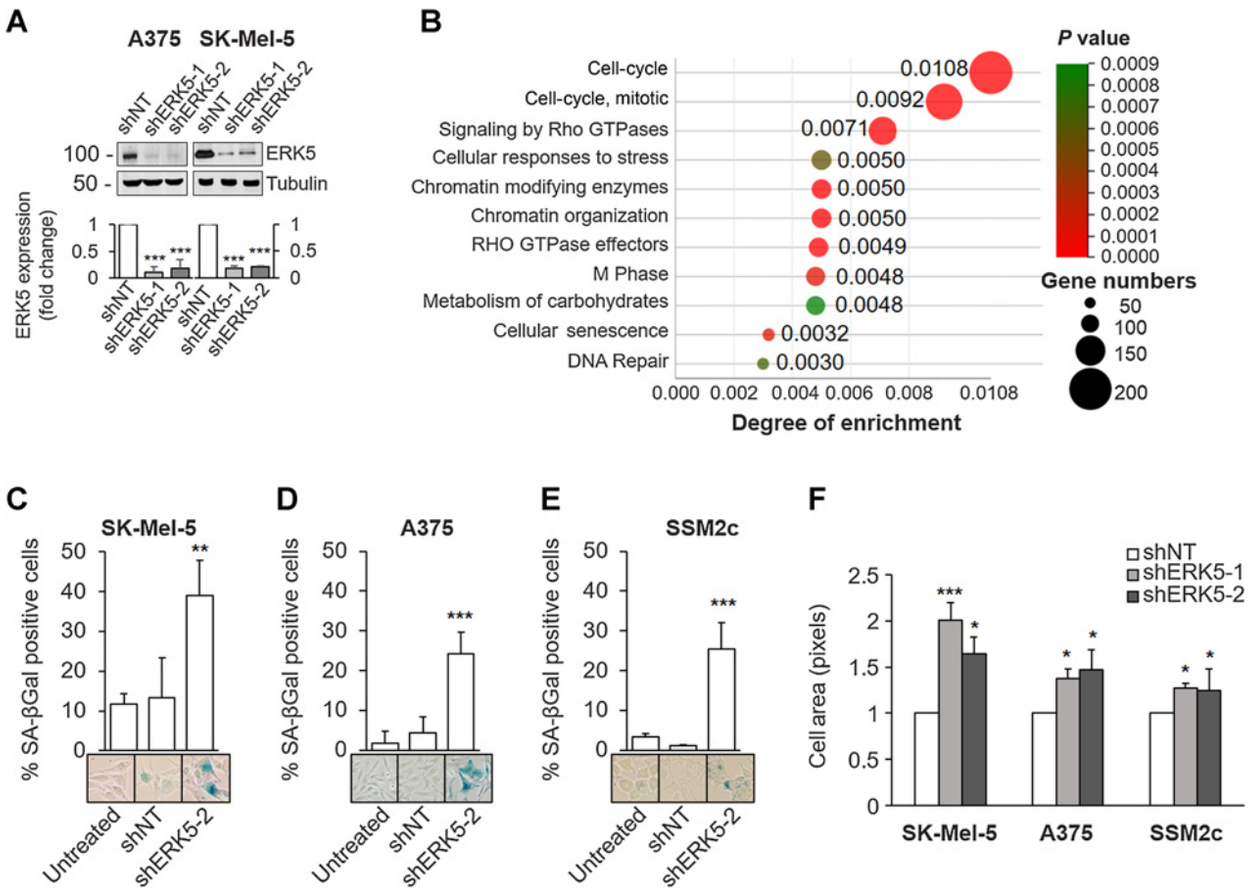

Figure 1.

ERK5 inhibition induces cellular senescence in melanoma cells. **A,** Genetic inhibition of ERK5. Cells were lysed after infection with lentiviral vectors carrying control nontargeting shRNA (shNT) or ERK5-specific shRNA (shERK5–1 and shERK5–2). Western blotting was performed with the indicated antibodies. Migration of molecular weight markers is indicated on the left (kDa). The graphs show average densitometric values of ERK5 protein levels normalized for tubulin content from three independent experiments. **B,** Transcriptomic analysis in A375 and SK-Mel-5 cells upon ERK5 KD. WebMeV analysis was performed on transcriptomic data after infection with lentiviral vectors carrying control or ERK5-specific shRNA. Data obtained from the two shRNA targeting ERK5 were averaged (A375, $n = 4$; SK-Mel-5, $n = 3$). Shown are the first eleven most impacted pathways based on degree of enrichment. Size of circles indicate the number of genes that are upregulated or downregulated in each pathway. **C–E,** ERK5 KD increased SA-βGal positivity in melanoma cells. Untreated cells or cells transduced with lentiviral vectors carrying control (shNT) or ERK5-specific shRNA (shERK5–2) were cultured for 72 hours. The percentage of SA-βGal–positive cells (blue ones) with respect to total number of cells/well was evaluated in three independent experiments. Representative images from each condition are shown. **F,** ERK5 KD induces an increase of melanoma cell area. Cell area was evaluated with ImageJ software. *P* values refer to differences with respect to shNT; *, $P < 0.05$; **, $P < 0.01$; ***, $P < 0.001$.

Table 1. Senescence and SASP-associated genes significantly deregulated in SK-Mel-5 and A375 melanoma cells upon ERK5 genetic inhibition. Data for shERK5 referred to average results from shERK5–1 and shERK5–2.

	A375		SK-Mel-5	
Gene symbol	Fold change shNT/shERK5	*P* value	Fold change shNT/shERK5	*P* value
HIST1H3B	−2.36	0.0178	−9.57	0.0252
HIST1H3F	−3.41	0.007	−5.96	0.0223
HIST1H4B	−2.61	0.0045	−2.25	0.0094
HIST1H4D	−1.7	0.0106	−4.7	0.0091
HIST1H4E	−2.45	0.0197	−2.35	0.0025
HIST1H4H	−2.85	0.0053	−2.13	0.0279
HIST1H4J	−1.88	0.0271	−2.9	0.0046
HIST1H4K	−1.75	0.0411	−2.9	0.0311
HIST2H3D	−1.8	0.0189	−1.7	0.0318
HIST2H4A	−1.8	0.0023	−9	0.0249
HIST2H4B	−1.88	0.0011	−4.3	0.0369
RBL1	−1.6	0.0389	−2.25	0.0159
LAMA1	−1.55	0.0306	−1.7	0.0194
CDC25A	−4.9	0.0063	−4.2	0.0022
LIN9	−1.6	0.004	−2.1	0.0078
CDKN1B	1.8	0.0136	2.04	0.05
CXCL1	6.7	0.0432	3.8	0.0496
CXCL8	20.3	0.0389	54.57	0.0434
CCL20	2	0.046	9.9	0.012
IGFBP7	7	0.0229	1.3	0.05
TP53	3.5	0.0189	1.6	0.028
RRAS	2.85	0.0000456	2.7	0.05
AKT3	2	0.008	1.96	0.03

previously (23, 24). Proteins were separated by SDS-PAGE and transferred onto Hybond PVDF (GE Healthcare) by electroblotting. Infrared imaging (Odyssey, Li-Cor Bioscience) was performed. Images were quantified with ImageJ software. Antibodies are in Supplementary Table S2.

RNA interference

TRC1.5-pLKO.1-puro lentiviral vectors (Supplementary Table S3) were produced in HEK293T cells as reported previously (25). Transduced cells were selected with 2 μg/mL puromycin for at least 72 hours.

Transcriptomic analysis

Total RNA was isolated using RNeasy Mini Kit (Qiagen), and mRNA expression evaluated with Affymetrix Clariom-S Human Genechip following the manufacturer's instructions. Transcriptome analysis console (TAC) software was used (fold change >1.5/<−1.5 and $P \leq 0.05$) to identify differentially expressed genes (DEG). Most enriched pathways were identified by Meta-analysis of DEG using WebMeV (Multiple Experiment Viewer).

Quantitative real-time PCR

Total RNA was isolated using TRIzol (Life Technologies). cDNA synthesis was carried out using ImProm-II Reverse Transcription System, while quantitative PCR (qPCR) was performed using GoTaq qPCR Master Mix (Promega Corporation). For primer sequences see Supplementary Material. QPCR was performed using CFX96 Touch Real-Time PCR Detection System (Bio-Rad). mRNA expression was normalized to GAPDH and 18S mRNA.

Flow cytometry

Cell-cycle phase distribution (propidium iodide staining) was determined as previously reported using a FACSCanto (Beckton Dickinson; ref. 26).

Chemokines determination in conditioned media

Fourteen days after lentiviral transduction, medium was replaced with DMEM/10% FBS. Conditioned media (CM) were harvested after 72 hours. Chemokine expression was measured in CM using RayBiotech Quantibody array (RayBiotech) following the manufacturer's instructions. Each antigen was measured in quadruplicate and relative fluorescence intensity determined using ImageJ software. Results were normalized for protein content in lysates.

Cell viability assay and neutralization experiments

Cell viability was measured by 3-(4,5-dimethylthiazol-2-yl)-3,5-diphenyltetrazolium bromide (MTT) assay. Cells were seeded in 96-well plate in DMEM/10% FBS. After 24 hours, medium was replaced with CM and cells further incubated for 72 hours. MTT (0.5 mg/mL) was added during the last 4 hours. Plates were read at 595 nm using a Microplate reader-550 (Bio-Rad). For neutralization experiments, control isotype IgG or neutralizing antibodies (Supplementary Table S2) were added to CM prior to administration to cells.

Determination of cellular senescence by senescence-associated βGal staining and of cell area

Cells were incubated for 72 hours and then fixed (2% formaldehyde, 10 minutes, room temperature). After washing, senescence-associated (SA) βGal staining solution (X-gal 1 mg/mL, 40 mmol/L citric acid, 5 mmol/L $C_6FeK_4N_6$, 5 mmol/L $C_6N_6FeK_3$, 150 mmol/L NaCl and 2 mmol/L $MgCl_2$; pH 6.1 -SK-Mel-5- or 5.9 -A375, SSM2c; ref. 27) was added (16 hours, 37°C). Senescent cell quantification was performed by counting SA-βGal–positive (blue) cells in 10 random images/well taken using a brightfield microscope. An average of 800 cells/condition were counted. In other experiments, cell area was evaluated with ImageJ software.

Immunohistochemistry and determination of cellular senescence *in vivo*

Formalin-fixed paraffin-embedded (FFPE) sections from archival xenografts established with shNT or shERK5–2 A375 or SSM2c cells, or with A375 cells from XMD8–92 (25 mg/kg)- or vehicle (2-hidroxypropyl-β-cyclodextrin 30%)-treated mice were used (15). Experiments had been approved by the Italian Ministry of Health (authorization no. 213/2015-PR) and were in accordance with the Italian ethic guidelines and regulations. Sections (3 μmol/L thick) were deparaffinized and stained with Sudan Black Blue (SBB; Bio-Optica) to reveal lipofuscin (28, 29), and counterstained with Nuclear Fast Red (NFR, Bio-Optica). Immunohistochemistry (IHC): After citrate buffer antigen retrieval, staining was performed with the UltraVision LP Detection System HRP Polymer Kit (Thermo Fisher Scientific) following the manufacturer's instructions. Sections were incubated overnight at 4°C with primary antibodies (Supplementary Table S2) and (3,3′-diaminobenzidine; Thermo Fisher Scientific; DAB) used as a chromogen. Sections were counterstained with hematoxylin.

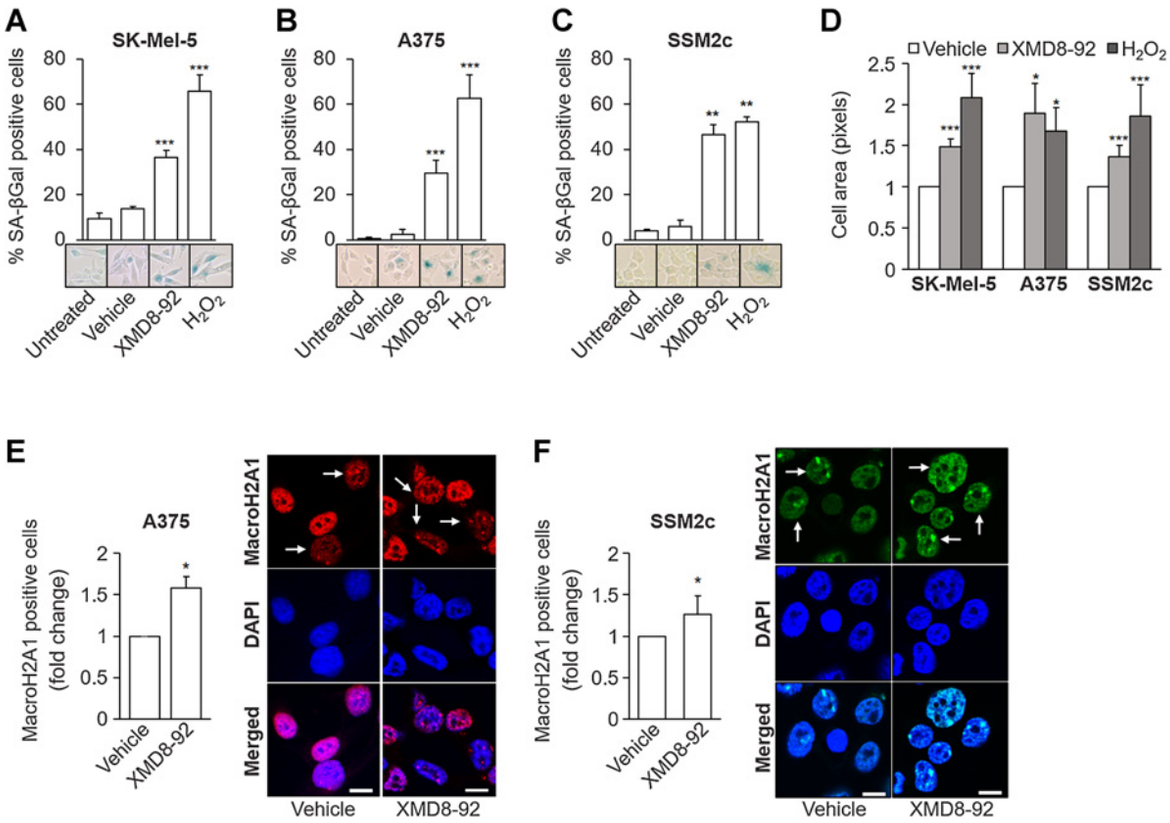

Figure 2.

Pharmacologic inhibition of ERK5 induces senescence in melanoma cells. **A–C,** Cells were left untreated or treated with DMSO (vehicle) or with 5 μmol/L XMD8–92 for 72 hours. Treatment with 300 nmol/L H_2O_2 during the first 2 hours was used as a positive control. The percentage of SA-βGal–positive cells (blue) with respect to the total number of cells/well was evaluated in three independent experiments. Representative images from each condition are shown. *P* values refer to differences with respect to vehicle-treated samples. **, $P < 0.01$; ***, $P < 0.001$. **D,** Pharmacologic inhibition of ERK5 induces an increase of melanoma cell area. The area of the cells was evaluated with ImageJ software. *P* values refer to differences with respect to shNT. *, $P < 0.05$; ***, $P < 0.001$. **E** and **F,** Pharmacologic inhibition of ERK5 induces an increase in macroH2A1-positive foci formation. Cells were treated with DMSO (vehicle) or with 5 μmol/L XMD8–92 for 72 hours and then stained for macroH2A1. Confocal images were analyzed to quantify macroH2A1-positive cells. *P* values refer to differences with respect to vehicle-treated cells. *, $P < 0.05$. Scale bar, 10 μm.

Colony formation assay

Cells were treated for 72 hours and then seeded in p60 dishes in DMEM 10% FBS. Colonies (i.e., more than 50 cells) were counted following crystal violet staining after 7 (A375) or 10 (SSM2c) days.

Immunofluorescence analysis

Cells were plated on glass coverslips and incubated for 72 hours in DMEM/2,5%FBS, and fixed with 4% paraformaldehyde (10 minutes, room temperature). Cells were permeabilized (0.2% Triton X-100) and saturated with 10% horse serum in PBS/1% BSA for 45 minutes. Incubation with primary antibody (overnight, 4°C) and with Cy2- or Cy3-labeled secondary antibodies was performed. Cell nuclei were labelled with DAPI (Invitrogen). Images were analyzed with a confocal inverted microscope equipped with a Nikon S Fluor 60× immersion oil objective (Nikon Instruments).

Statistical analysis

Data represent mean or ± SD values calculated on at least three independent experiments. *P* values were calculated using Student *t* test (two groups) or one-way ANOVA (more than two groups). $P < 0.05$ was considered statistically significant.

Results

ERK5 inhibition induces cellular senescence in melanoma cells and xenografts

We previously showed that ERK5 inhibition reduces proliferation of melanoma cells *in vitro* and growth of melanoma xenografts *in vivo* (15). To deepen the role of ERK5 in melanoma growth, we performed transcriptomic experiments in BRAFV600E A375 and SK-Mel-5 melanoma cells after ERK5 KD with two different shRNAs (**Fig. 1A**). DEG analysis showed that the most impacted pathways dealt with cell-cycle regulation. Interestingly, cellular senescence was the tenth most impacted pathway (0.0032 degree of enrichment; **Fig. 1B**; Supplementary Table S4). We also identified several senescence-related genes, whose expression was significantly changed upon ERK5 KD (**Table 1**).

We then verified whether ERK5 inhibition elicits cellular senescence. Both SK-Mel-5 and A375 ERK5-KD cells showed a marked increase (20%–30%) of SA-βGal–positive cells, when compared with naïve or to control nontargeting shRNA-transduced cells (**Fig. 1C** and **D**). The same effects were observed in triple wild-type SSM2c cells (**Fig. 1E**). In all three cell lines, ERK5 KD determined an increase of the cell area (**Fig. 1F**), a morphologic change typical of senescent cells (16). Importantly, the ERK5 inhibitors XMD8–92 (**Fig. 2A–C**)

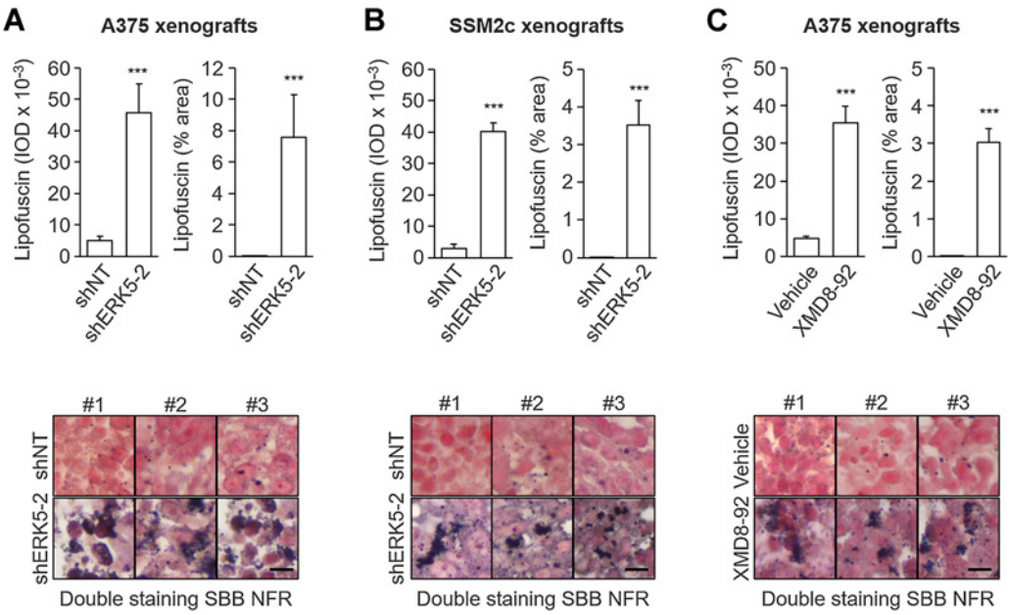

Figure 3.

Genetic inhibition of ERK5 induces senescence in human melanoma xenografts. **A–C,** FFPE sections from A375 (**A**) and SSM2c (**B**) shNT and shERK5–2 xenografts or A375 xenografts obtained from mice treated with vehicle or XMD8–92 (**C**) were stained with Sudan Black B (SBB) to evaluate lipofuscin content and Nuclear Fast Red (NFR). Integrated optical density (IOD; left graphs) or percentage (%) of area of positively stained tissues (right graphs) was used to quantify the amount of lipofuscin. The integrated optical density and percent area was calculated from six different ×40 magnified fields from three xenografts. Representative images are shown. Scale bar, 40 μm. ***, $P < 0.001$.

and JWG-045 (Supplementary Fig. S1A and S1B), used at concentrations with negligible off-target effects (15), as well as JWG-071 (Supplementary Fig. S1A), a more specific inhibitor of ERK5 over bromodomain-containing proteins (30, 31), were able to induce cellular senescence. Interestingly, the MEK5 inhibitor BIX02189 did not induce cellular senescence (Supplementary Fig. S1A–S1C). Pharmacologic inhibition of ERK5, which lasted for the entire duration of the experiments (Supplementary Fig. S1D), determined an increase of cell area (**Fig. 2D**), and of senescence-associated heterochromatin foci (SAHF)-positive cells (**Fig. 2E** and **F**). The latter effect was also observed after ERK5 KD (Supplementary Fig. S1E). The BRAFV600E inhibitor vemurafenib, but not the MEK1/2 inhibitor trametinib, determined an increase of senescent cells similarly to XMD8–92, and in combination with the latter further increased the percentage of senescent cells (Supplementary Fig. S1F).

The occurrence of cellular senescence *in vivo* was then investigated performing lipofuscin staining on archival xenografts of A375 and SSM2c cells transduced with shNT- or shERK5-encoding lentiviral vectors, the latter of which drastically reduced tumor growth (Supplementary Fig. S2A and S2B; ref. 15). In A375 and SSM2c xenografts, the amount of lipofuscin and the percentage of lipofuscin-stained area were markedly higher in ERK5-KD than in control xenografts (**Fig. 3A** and **B**). Similarly, systemic administration of XMD8–92, which induced a marked reduction of tumor growth (Supplementary Fig. S2C; ref. 15), determined a robust increase of lipofuscin in A375 xenografts with respect to vehicle-treated mice (**Fig. 3C**).

ERK5 inhibition impairs cell-cycle progression and affects cell-cycle regulators in melanoma cells

We then deepened the effects of ERK5 inhibition on cell-cycle progression that is impaired in senescent cells characterized by an irreversible block of proliferation. ERK5 KD determined an increase of cells in G_0–G_1 or G_2–M phase in A375 or SSM2c cells, respectively (**Fig. 4A** and **B**). This increase is robust when taking into consideration that 20% to 30% of the population undergoes senescence upon ERK5 KD (**Fig. 1C–E**). ERK5 KD determined a reduction of PCNA protein, in keeping with a reduced proliferation (Supplementary Fig. S3). Moreover, exposure to mitogens (i.e., 10% FBS), that increased the percentage of vehicle-treated cells in S phase, did not affect cell-cycle phase distribution in XMD8-92–treated cells (**Fig. 4C** and **D**). Of note, XMD8–92 blocked cell-cycle progression with a significant increase of cells in G_0–G_1 or G_2–M phase in A375 and SSM2c cells, respectively, in line with ERK5-KD cell results (**Fig 4A** and **B**) and with our previous data (15). Colony assay experiments using 72 hours XMD8-92–treated cells demonstrated their irreversible inability to proliferate (**Fig. 4E** and **F**).

The cyclin-dependent kinase inhibitor p21 mediates cellular senescence induced by ERK5 inhibition

To deepen the impact of ERK5 inhibition on cell-cycle regulators involved in senescence, we first revealed that ERK5 KD determined a reduction of RB phosphorylation and an increase of the cyclin-dependent kinase inhibitor (CDKi) p21 protein level in A375 and SSM2c cells (**Fig. 5A**), both representing the most used markers of cellular senescence. Furthermore, we found a reduced expression of cyclin E, D1, and A2 (**Fig. 5A**), in keeping with a reduced proliferation. Interestingly, either genetic (**Fig. 5A** and **B**) or pharmacologic (**Fig. 5C** and **D**) ERK5 inhibition increased the amount of the CDKi p14 protein. The increased protein levels of p21 (**Fig. 5E** and **F**) and of p14 (**Fig. 5G** and **H**) upon ERK5 KD were confirmed *in vivo* using A375 and SSM2c xenografts. Of note, the increase in the percentage of p14 positive cells in ERK5-KD A375 xenografts, although significant,

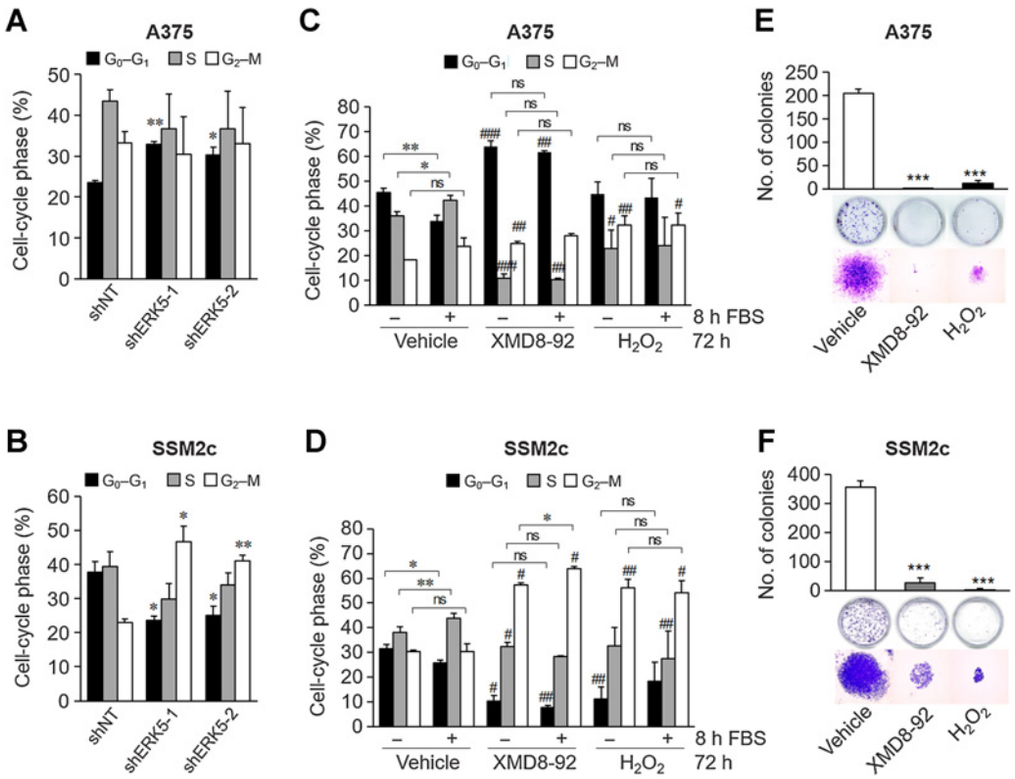

Figure 4.

Effects of ERK5 inhibition on cell-cycle progression and colony formation ability. **A** and **B,** Cells were transduced with lentiviral vectors carrying control (shNT) or ERK5-specific shRNA (shERK5–1 or shERK5–2) and were cultured for 72 hours. Cell-cycle phase distribution was then determined in three independent experiments. *P* values refer to differences with respect to shNT cells. *, $P < 0.05$; **, $P < 0.01$. **C** and **D,** Cells were treated with vehicle or 5 μmol/L XMD8–92 for 72 hours. Treatment with 300 nmol/L H_2O_2 during the first 2 hours was used as a positive control. After 72 hours, cells were treated with 10% FBS for 8 hours or left untreated. Cell-cycle phase distribution was then determined in three independent experiments. **#**, $P < 0.05$; **##**, $P < 0.01$; **###**, $P < 0.001$ refer to differences with vehicle-treated samples; *, $P < 0.05$; **, $P < 0.01$. **E** and **F,** Cells were treated with vehicle or 5 μmol/L XMD8–92 for 72 hours. Treatment with 300 nmol/L H_2O_2 during the first 2 hours was used as a positive control. After 72 hours, colony-forming assay was performed. *P* values refer to differences with respect to vehicle-treated cells. ***, $P < 0.001$. ns, nonsignificant.

was relatively low (**Fig. 5G**), and, accordingly, the increased amount of p14 protein was appreciable in nuclear extracts only (**Fig. 5A–C**). Consistently, we observed an increase of p21 and a decrease of PCNA-positive A375 cells after treatment with XMD8–92 *in vivo* (Supplementary Fig. S4A and S4B). Upon ERK5 KD, we also confirmed the increase of p27 and p53 protein levels, and the reduction of RBL-1 mRNA, identified by the transcriptomic analysis (**Table 1**). Moreover, the increased phosphorylation of CDK1 at Y15 seems to support the observed reduction of phosphatase CDC25a expression (Supplementary Fig. S4C–S4E).

Among the cell-cycle regulators, whose expression is markedly deregulated upon ERK5 inhibition, we focused on p21 in order to deepen the mechanism of ERK5 KD-associated senescence. Of note, p53 was found increased in the transcriptomic data (and confirmed at the protein level), and p21 is the effector of the majority of p53-induced biological effects including cellular senescence. Genetic inhibition of p21 using two different shRNAs (**Fig. 6A**) halved the percentage of A375 cells undergoing cellular senescence following treatment with XMD8-92 or H_2O_2 (**Fig. 6B**), revealing a key role of p21 in ERK5-dependent cellular senescence. The observed reduction of the percentage of cells undergoing senescence upon p21 KD was robust, taking into consideration that XMD8-92 induced a slight but significant increase of p21 protein level in p21 KD cells (**Fig. 6C**; compare lanes 5 and 6 vs. 2 and 3, respectively). In this respect, the lack of effect of BIX02189 on cellular senescence (Supplementary Fig. S1A–S1C) is in keeping with the ineffectiveness of this compound in increasing p21 protein level (15), while XMD8-92 induced a dose dependent increase of cellular senescence and p21 protein (Supplementary Fig. S5A–S5C). The above data indicate that cellular senescence induced by ERK5 inhibition in melanoma cells relies, at least in part, on p21.

ERK5 inhibition induces the senescence-associated secretory phenotype

One of the key features of senescent cells is the senescence-associated secretory phenotype (SASP; ref. 32). Transcriptomic data showed that SASP (0.0020 degree of enrichment, Supplementary Table S4) and SASP-related genes (**Table 1**) were significantly modulated upon ERK5 KD. Among the latter, transcriptomic analysis indicated that CXCL1/GROalpha and CXCL8/IL8, two of the most prominent SASP products (33), and CCL20/MIP3alpha mRNA were significantly upregulated in both A375 and SK-Mel-5 ERK5-KD cells (**Fig. 7A**). IL6, another key component of the SASP, was not altered upon ERK5 KD (**Fig. 7A**). QPCR experiments confirmed that lack of increase of IL6 mRNA in the same experimental settings in which CXCL8 mRNA was significantly increased in A375, SK-Mel-5, and SSM2c ERK5-KD cells (**Fig. 7B**). Importantly, protein array in CM

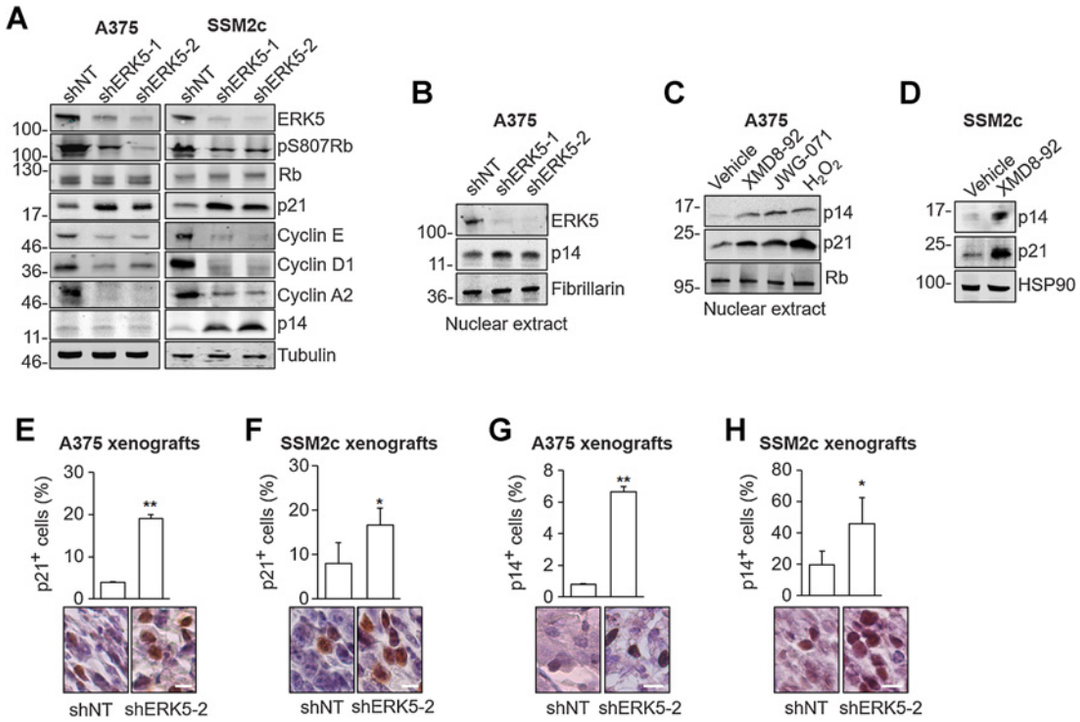

Figure 5.

Effects of ERK5 inhibition on signaling molecules involved in cell cycle and senescence. **A,** Cells transduced with control nontargeting shRNA (shNT) or ERK5-specific shRNAs (shERK5–1 and shERK5–2) were lysed, and Western blotting was performed with the indicated antibodies. Images are representative of three independent experiments showing similar results. Migration of molecular weight markers is indicated on the left (kDa). **B,** Cells transduced with control nontargeting shRNA (shNT) or ERK5-specific shRNAs (shERK5–1 and shERK5–2) were lysed, and Western blotting was performed on nuclear extracts with the indicated antibodies. Images are representative of three independent experiments showing similar results. Migration of molecular weight markers is indicated on the left (kDa). **C,** Cells were treated with DMSO (vehicle) or with the indicated drugs (5 μmol/L) for 72 hours. Treatment with 300 nmol/L H_2O_2 during the first 2 hours was used as a positive control. Cells were lysed, and Western blotting was performed on nuclear extracts with the indicated antibodies. Migration of molecular weight markers is indicated on the left (kDa). **D,** Cells were treated with DMSO (vehicle) or with XMD8–92 (5 μmol/L) for 72 hours. Cells were lysed, and Western blotting was performed with the indicated antibodies. Images are representative of three independent experiments showing similar results. Migration of molecular weight markers is indicated on the left (kDa). **E–H,** IHC detection of p21 (**E** and **F**) or p14 (**G** and **H**) proteins in shNT- or shERK5–2 xenografts. Hematoxylin counterstaining was performed. Bar plots of percentage (%) of p21 (**E** and **F**)- or p14 (**G** and **H**)-positive cells are shown. The percentage of positive cells was calculated from six different ×40 magnified fields from three shNT and three shERK5–2 tumors. Representative photographs are shown (original magnification, ×40). Scale bar, 40 μm.

(**Fig. 7C**) confirmed that CXCL1, CXCL8, and CCL20 protein levels were significantly increased in ERK5-KD A375 cells. Interestingly, publicly available datasets from the cBioPortal for Cancer Genomics (34, 35) confirmed the coexpression of the above-mentioned SASP products in patients with melanoma (Supplementary Fig. S6A and S6B). Indeed, the amount of CXCL1/GROalpha mRNA showed a robust positive correlation with that of CXCL8 (0.58 Spearman correlation; $P = 6.68e^{-41}$), and with that of CCL20 (0.49 Spearman correlation; $P = 1.34e^{-27}$; Skin Cutaneous Melanoma TCGA, Pan-Cancer Atlas; Supplementary Fig. S6A). The positive correlation between the mRNA level of CXCL1/GROalpha and of CXCL8 was confirmed (0.35 Spearman correlation; $P = 0.028$) in another data set (Metastatic Melanoma, DFCI, Science 201; Supplementary Fig. S6B; ref. 36).

SASP products may elicit either pro- or antiproliferative effects on tumor cells (29). To discriminate between these possible opposite outcomes, we tested CM from A375 and SK-Mel-5 cells and found that CM recovered from ERK5-KD cells markedly reduced the viability of either A375 or SK-MEL-5 cells with respect to CM from shNT cells (**Fig. 7D**). The proof that CXCL1, CXCL8, and CCL20 are among the SASP products responsible for the reduced proliferation was obtained using neutralizing antibodies (**Fig. 7E**). Indeed, each blocking antibody was able to partially rescue melanoma cell proliferation.

Discussion

Cellular senescence is considered a potent suppressive mechanism of tumorigenesis, and therapies that enhance senescence, besides promoting a stable cell growth arrest, may stimulate the activation of the antitumor immune response. Based on that, prosenescence molecules are actively sought after in view of their potential use as antineoplastic treatments (12, 13). In this study, we demonstrated a prominent role of ERK5 in cellular senescence in human melanoma. In BRAF-mutated and wild-type melanoma cells and xenografts, ERK5 inhibition induced indeed marked cellular senescence and production of several soluble mediators involved in the SASP. Mechanistically, we demonstrated that ERK5-dependent senescence is mediated by the CDKi p21.

The induction of cellular senescence upon ERK5 inhibition was demonstrated using different approaches. Senescence emerged first, in transcriptomic experiments, as one of the most impacted pathways upon ERK5 KD in BRAFV600E-mutated melanoma cells. Besides

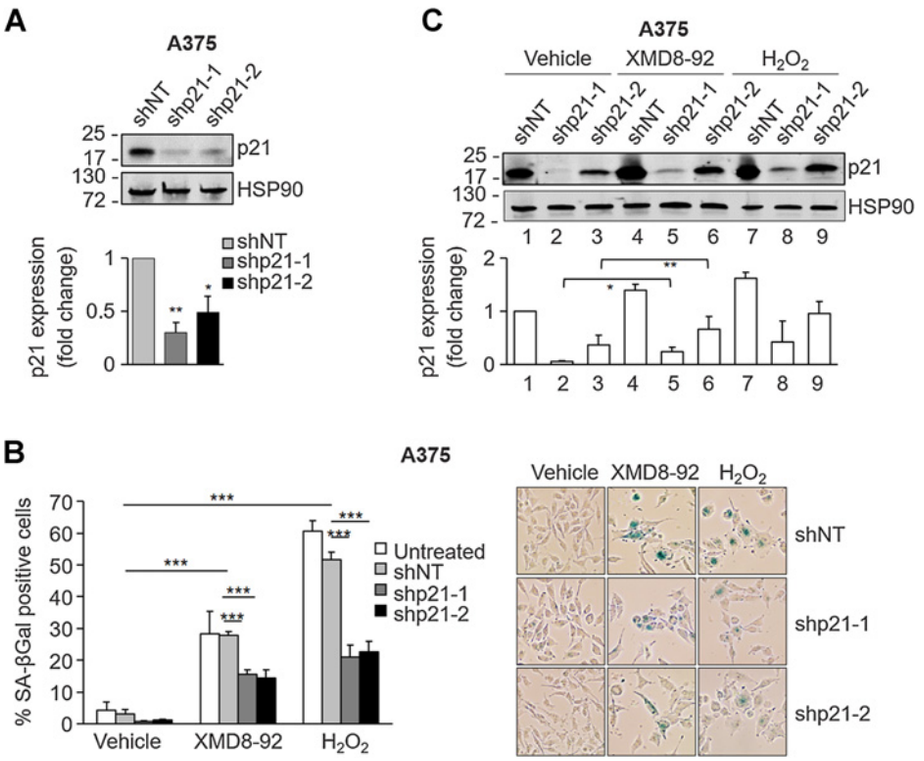

Figure 6.

Genetic inhibition of p21 prevents cellular senescence induced by ERK5 inhibition in A375 cells. **A,** Genetic inhibition of p21. Cells transduced with control nontargeting shRNA (shNT) or p21-specific shRNA (shp21–1 and shp21–2) were lysed, and Western blotting was performed with the indicated antibodies. Migration of molecular weight markers is indicated on the left (kDa). The graph shows average densitometric values of p21 protein normalized for HSP90 content from three independent experiments. **B,** Parental A375 (untreated) or A375 infected with lentiviral vectors carrying shNT, shp21–1, or shp21–2 were treated with DMSO (vehicle) or with XMD8–92 (5 μmol/L) for 72 hours. Treatment with 300 nmol/L H_2O_2 during the first 2 hours was used as a positive control. The percentage of SA-βGal-positive cells with respect to the total number of cells/well was evaluated in three independent experiments. Representative images from each condition are shown. **C,** A375 cells infected with lentiviral vectors carrying shNT, shp21–1, or shp21–2 were treated with DMSO (vehicle) or 5 μmol/L XMD8–92 for 72 hours and H_2O_2 (300 nmol/L for 2 hours) and then lysed. p21 expression was evaluated by Western blotting. Blots are representative of three independent experiments showing similar results. The graph shows average densitometric values of p21 protein normalized for HSP90 content. *, $P < 0.05$; **, $P < 0.01$; ***, $P < 0.001$.

cellular senescence, ERK5 inhibition significantly impacted oxidative stress induced senescence and the SASP. In this respect, ERK5 had been previously reported to be activated in colorectal adenocarcinoma cells undergoing methotrexate-induced senescence (37). We demonstrated the occurrence of cellular senescence by showing that both genetic and pharmacologic inhibition of ERK5 determined a marked increase of SA-βGal positivity in melanoma cells harboring wild-type or oncogenic BRAF, as well as of cellular area and of SAHF. In addition, we found that the expression of a number of genes known to regulate cell cycle and cellular senescence, including CDC25a, RBL-1, p27, and p53, was altered upon ERK5 KD.

Cellular senescence upon ERK5 inhibition was also demonstrated *in vivo*. Indeed, in A375 and SSM2c xenografts, ERK5 KD determined a robust increase of lipofuscin, an indicator of cellular senescence *in vivo* (28). More importantly in view of a possible translation to the clinics, similar effects were observed in melanoma xenografts of XMD8-92–treated mice. The occurrence of a block of cell-cycle progression, an event invariably linked to cellular senescence (16), was supported by the fact that ERK5-KD cells underwent an accumulation in G_0–G_1 or G_2–M phase, depending on the cell line, and cells treated with XMD8-92 showed reduced ability to respond to mitogens and did not form colonies upon replating. Consistently, ERK5 inhibition determined a reduction of RB phosphorylation and cyclin protein levels, as well as an increase of p21 protein. This CDKi was identified as a prominent player of ERK5-dependent cellular senescence. Indeed, the amount of p21 protein was increased following ERK5 pharmacologic inhibition, whereas p21 genetic inhibition reverted the prosenescence effect of XMD8-92 treatment. While the involvement of p21 in ERK5-mediated biological effects has been widely reported (21, 38), the role of p21 in ERK5-mediated cellular senescence is a novel finding.

Cellular senescence may be accompanied by the SASP, which consists of secretion of a number of soluble factors in the surrounding microenvironment. SASP determines both beneficial and deleterious biological outcomes, which makes of senescence a double-edged sword with respect to cancer onset and development (32, 39). In this work, we identified a number of SASP-related chemokines, including CXCL1, CXCL8, and CCL20, that are markedly increased in CM of ERK5-KD cells undergoing cellular senescence. Our data showed that these CM markedly reduced the viability of melanoma cells, and that the treatment with neutralizing antibodies for each of the above chemokines rescued the proliferation of melanoma cells. In this respect, despite the growth-promoting functions of CXCL8, CXCL1, and CCL20 reported so far (40–44) may appear in contrast with the

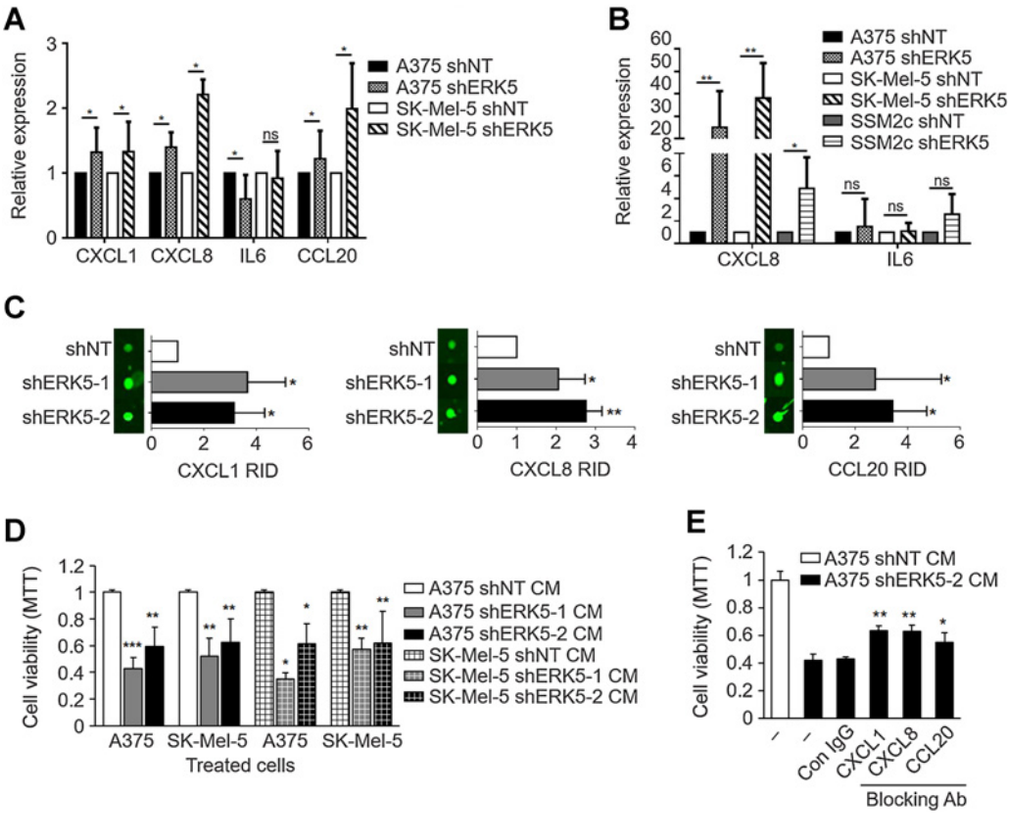

Figure 7.

ERK5 KD increases SASP soluble factors. **A,** mRNA expression profiles were determined using TAC software. Data shown for shERK5 are mean (±SD) of pulled data from shERK5–1 and shERK5–2 (A375, $n = 4$; SK-Mel-5, $n = 3$). *, $P < 0.05$ as determined using one-way ANOVA. **B,** CXCL8 and IL6 mRNA levels determined by qPCR in ERK5 KD cells. Data shown for shERK5 are mean (±SD) of pulled data from shERK5–1 and shERK5–2 (A375, $n = 6$; SK-Mel-5, $n = 6$). **C,** Chemokines expression in CM from ERK5-KD (shERK5–1 and shERK5–2) A375 cells was analyzed using Quantibody Human Array (#QAA-CUST-SW; RayBiotech). Each antigen was measured in quadruplicate from three independent experiments and the relative fluorescence intensity (RID) was determined using ImageJ software (NIH). The obtained results were normalized for protein content in cell lysates. Data shown are mean ± SD. Representative fluorescent dots are shown. **D,** MTT was performed in A375 or SK-Mel-5 cells treated with CM harvested from A375 or SK-Mel-5 cells 14 days posttransduction with shNT or shERK5 (shERK5–1 or shERK5–2) lentiviral vectors. Data shown are mean ± SD from three independent experiments. **E,** MTT was performed on A375 cells treated with CM harvested from shNT (white column) or shERK5–2 (dark columns) A375 cells in the presence of 10 μg/mL of the indicated blocking antibodies or control IgG. Data shown are mean ± SD from three independent experiments. *, $P < 0.05$; **, $P < 0.01$; ***, $P < 0.001$ as determined by Student t test. ns, nonsignificant.

antiproliferative effects elicited by CM from ERK5-KD cells, it has been demonstrated that senescent cells may activate a self-amplifying secretory network in which CXCR2-binding chemokines (i.e., CXCL1 and CXCL8) reinforce growth arrest (45). As regard the link between ERK5 inhibition and SASP occurrence, multiple different nuclear and cytoplasmic factors have been shown to trigger SASP, including chromatin remodeling and SAHF formation. In this respect, it is worth pointing out that ERK5 KD determined a profound remodeling of the mRNA levels of a number of histone variants, as well as SAHF increase. However, the molecular mechanism linking ERK5 KD to chemokine regulation remains to be investigated.

Another relevant finding of our study is the identification of prosenescence drugs that may be exploited for cancer treatment. Indeed, XMD8-92, JWG-045, and JWG-071 elicited robust senescence in melanoma cells. The fact that XMD8-92, extensively showed to reduce tumor growth *in vitro* and *in vivo* (8), has off-target effects (46) does not reduce the possibility to exploit this small-molecule inhibitor as a prosenescence drug. Interestingly, the prosenescence effect of XMD8-92 was increased when used in combination with vemurafenib, that we found able to induce senescence in melanoma cells, in keeping with a previous report (47). Thus, combined targeting of BRAF and ERK5, besides reducing tumor growth more efficiently than single treatments (15), supports prosenescent signals. These effects are in line with the well-established fact that, either chemo and radio, as well as targeted therapies engage a senescence response as part of the outcome (13). However, if this combination is more effective in preventing resistance mechanisms with respect to BRAF/MEK inhibitors alone remains to be investigated.

Authors' Disclosures

No disclosures were reported.

Authors' Contributions

A. Tubita: Data curation, formal analysis, investigation, writing–original draft, writing–review and editing. **Z. Lombardi:** Data curation, formal analysis, investigation, methodology, writing–original draft, writing–review and editing. **I. Tusa:** Data curation, formal analysis, supervision, writing–original draft, writing–review and editing. **A. Lazzeretti:** Formal analysis, methodology. **G. Sgrignani:** Formal analysis. **D. Papini:** Formal analysis. **A. Menconi:** Formal analysis. **S. Gagliardi:**

Investigation. **M. Lulli:** Data curation, investigation. **P. Dello Sbarba:** Resources, writing–review and editing. **A. Esparís-Ogando:** Resources, writing–review and editing. **A. Pandiella:** Resources, writing–review and editing. **B. Stecca:** Investigation, writing–review and editing. **E. Rovida:** Conceptualization, resources, data curation, formal analysis, supervision, funding acquisition, investigation, writing–original draft, project administration, writing–review and editing.

Acknowledgments

The work in E. Rovida's lab was supported by grants from Associazione Italiana per la Ricerca sul Cancro (AIRC, IG-15282 and IG-21349), by Ente Fondazione Cassa di Risparmio di Firenze (ECRF), and Università degli Studi di Firenze (Fondo di Ateneo ex-60%). A. Tubita was supported by a "Carlo Zanotti" Fondazione Italiana per la Ricerca sul Cancro (FIRC)-AIRC fellowship (ID-23847).

The costs of publication of this article were defrayed in part by the payment of page charges. This article must therefore be hereby marked *advertisement* in accordance with 18 U.S.C. Section 1734 solely to indicate this fact.

Received April 10, 2021; revised October 6, 2021; accepted November 15, 2021; published first November 19, 2021.

References

1. Balch CM, Gershenwald JE, Soong SJ, Thompson JF, Atkins MB, Byrd DR, et al. Final version of 2009 AJCC melanoma staging and classification. J Clin Oncol 2009;27:6199–06.
2. Hodis E, Watson IR, Kryukov GV, Arold ST, Imielinski M, Theurillat JP, et al. A landscape of driver mutations in melanoma. Cell 2012;150:251–63.
3. Cohen ED, Mariol MC, Wallace RMH, Weyers J, Kamberov YG, Pradel J, et al. DWnt4 regulates cell movement and focal adhesion kinase during drosophila ovarian morphogenesis. Dev Cell 2002;2:437–48.
4. Chapman PB, Hauschild A, Robert C, Haanen JB, Ascierto P, Larkin J, et al. Improved survival with vemurafenib in melanoma with BRAF V600E mutation. N Engl J Med 2011;364:2507–16.
5. Samatar AA, Poulikakos PI. Targeting RAS-ERK signalling in cancer: promises and challenges. Nat Rev Drug Discov 2014;13:928–42.
6. Tubita A, Tusa I, Rovida E. Playing the whack-a-mole game: ERK5 activation emerges among the resistance mechanisms to RAF-MEK1/2-ERK1/2- targeted therapy. Front Cell Dev Biol 2021;9:647311.
7. Drew BA, Burow ME, Beckman BS. MEK5/ERK5 pathway: the first fifteen years. Biochim Biophys Acta 2012;1825:37–48.
8. Stecca B, Rovida E. Impact of ERK5 on the hallmarks of cancer. Int J Mol Sci 2019;20:1426.
9. Gomez N, Erazo T, Lizcano JM. ERK5 and cell proliferation: nuclear localization is what matters. Front Cell Dev Biol 2016;22; 4:105.
10. Tubita A, Lombardi Z, Tusa I, Dello Sbarba P, Rovida E. Beyond kinase activity: ERK5 nucleo-cytoplasmic shuttling as a novel target for anticancer therapy. Int J Mol Sci 2020;21:938.
11. Campisi J. Cellular senescence as a tumor-suppressor mechanism. Trends Cell Biol 2001;11:S27–31.
12. Acosta JC, Gil J. Senescence: a new weapon for cancer therapy. Trends Cell Biol 2012;22:211–9.
13. Nardella C, Clohessy JG, Alimonti A, Pandolfi PP. Pro-senescence therapy for cancer treatment. Nat Rev Cancer 2011;11:503–11.
14. Gray-Schopfer V, Wellbrock C, Marais R. Melanoma biology and new targeted therapy. Nature 2007;445:851–7.
15. Tusa I, Gagliardi S, Tubita A, Pandolfi S, Urso C, Borgognoni L, et al. ERK5 is activated by oncogenic BRAF and promotes melanoma growth. Oncogene 2018; 37:2601–14.
16. Muñoz-Espín D, Serrano M. Cellular senescence: from physiology to pathology. Nat Rev Mol Cell Biol 2014;15:482–96.
17. Anerillas C, Abdelmohsen K, Gorospe M. Regulation of senescence traits by MAPKs. Geroscience 2020;42:397–408.
18. Giard DJ, Aaronson SA, Todaro GJ, Arnstein P, Kersey JH, Dosik H, et al. In vitro cultivation of human tumors: establishment of cell lines derived from a series of solid tumors. J Natl Cancer Inst 1973;51:1417–23.
19. Carey TE, Takahashi T, Resnick LA, Oettgen HF, Old LJ. Cell surface antigens of human malignant melanoma: mixed hemadsorption assays for humoral immunity to cultured autologous melanoma cells. Proc Natl Acad Sci U S A 1976;73: 3278–82.
20. Pandolfi S, Montagnani V, Penachioni JY, Vinci MC, Olivito B, Borgognoni L, et al. WIP1 phosphatase modulates the hedgehog signaling by enhancing GLI1 function. Oncogene 2013;32:4737–47.
21. Yang Q, Deng X, Lu B, Cameron M, Fearns C, Patricelli MP, et al. Pharmacological inhibition of BMK1 suppresses tumor growth through promyelocytic leukemia protein. Cancer Cell 2010;18:258–67.
22. Tatake RJ, O'Neill MM, Kennedy CA, Wayne AL, Jakes S, Wu D, et al. Identification of pharmacological inhibitors of the MEK5/ERK5 pathway. Biochem Biophys Res Commun 2008;377:120–5.
23. Rovida E, Spinelli E, Sdelci S, Barbetti V, Morandi A, Giuntoli S, et al. ERK5/BMK1 is indispensable for optimal colony-stimulating factor 1 (CSF-1)-induced proliferation in macrophages in a src-dependent fashion. J Immunol 2008;180: 4166–72.
24. Barbetti V, Morandi A, Tusa I, Digiacomo G, Riverso M, Marzi I, et al. Chromatin-associated CSF-1R binds to the promoter of proliferation-related genes in breast cancer cells. Oncogene 2014;33:4359–64.
25. Rovida E, Di Maira G, Tusa I, Cannito S, Paternostro C, Navari N, et al. The mitogen-activated protein kinase ERK5 regulates the development and growth of hepatocellular carcinoma. Gut 2015;64:1454–65.
26. Barbetti V, Tusa I, Cipolleschi MG, Rovida E. Dello sbarba P. AML1/ETO sensitizes via TRAIL acute myeloid leukemia cells to the pro-apoptotic effects of hypoxia. Cell Death Dis 2013;4:e536.
27. Zhao J, Fuhrmann-Stroissnigg H, Gurkar AU, Flores RR, Dorronsoro A, Stolz DB, et al. Quantitative analysis of cellular senescence in culture and *in vivo*. Curr Protoc Cytom 2017;79:9.51.1–9.51.25.
28. Georgakopoulou EA, Tsimaratou K, Evangelou K, Fernandez Marcos PJ, Zoumpourlis V, Trougakos IP, et al. Specific lipofuscin staining as a novel biomarker to detect replicative and stress-induced senescence. a method applicable in cryo-preserved and archival tissues. Aging 2013;5: 37–50.
29. Evangelou K, Gorgoulis VG. Sudan black B, the specific histochemical stain for lipofuscin: a novel method to detect senescent cells. Methods Mol Biol 2017;1534: 111–9.
30. Wang J, Erazo T, Ferguson FM, Buckley DL, Gomez N, Muñoz-Guardiola P, et al. Structural and atropisomeric factors governing the selectivity of pyrimido-benzodiazipinones as inhibitors of kinases and bromodomains. ACS Chem Biol 2018;13:2438–48.
31. Williams CA, Fernandez-Alonso R, Wang J, Toth R, Gray NS, Findlay GM. Erk5 is a key regulator of naive-primed transition and embryonic stem cell identity. Cell Rep 2016;16:1820–8.
32. Coppé JP, Desprez PY, Krtolica A, Campisi J. The senescence-associated secretory phenotype: the dark side of tumor suppression. Annu Rev Pathol 2010;5:99–118.
33. Coppé JP, Patil CK, Rodier F, Sun Y, Muñoz DP, Goldstein J, et al. Senescence-associated secretory phenotypes reveal cell-nonautonomous functions of oncogenic RAS and the p53 tumor suppressor. PLoS Biol 2008;6:2853–68.
34. Cerami E, Gao J, Dogrusoz U, Gross BE, Sumer SO, Aksoy BA, et al. The cBio cancer genomics portal: an open platform for exploring multidimensional cancer genomics data. Cancer Discov 2012;2:401–4.
35. Gao XJ, Potter CJ, Gohl DM, Silies M, Katsov AY, Clandinin TR, et al. Specific kinematics and motor-related neurons for aversive chemotaxis in drosophila. Curr Biol 2013;23:1163–72.
36. Van Allen EM, Miao D, Schilling B, Shukla SA, Blank C, Zimmer L, et al. Genomic correlates of response to CTLA-4 blockade in metastatic melanoma. Science 2015;350:207–1.
37. Dabrowska M, Skoneczny M, Rode W. Functional gene expression profile underlying methotrexate-induced senescence in human colon cancer cells. Tumour Biol 2011;32:965–76.
38. Perez-Madrigal D, Finegan KG, Paramo B, Tournier C. The extracellular-regulated protein kinase 5 (ERK5) promotes cell proliferation through the down-regulation of inhibitors of cyclin dependent protein kinases (CDKs). Cell Signal 2012;24:2360–8.
39. Wang B, Kohli J, Demaria M. Senescent cells in cancer therapy: friends or foes? Trends Cancer 2020;6:838–57.

40. Green D, Eyre H, Singh A, Taylor JT, Chu J, Jeys L, et al. Targeting the MAPK7/MMP9 axis for metastasis in primary bone cancer. Oncogene 2020;39:5553–69.
41. Finegan KG, Perez-Madrigal D, Hitchin JR, Davies CC, Jordan AM, Tournier C. ERK5 is a critical mediator of inflammation-driven cancer. Cancer Res 2015;75:742–53.
42. Pereira DM, Gomes SE, Borralho PM, Rodrigues CMP. MEK5/ERK5 activation regulates colon cancer stem-like cell properties. Cell Death Discov 2019;5:68.
43. Bar-Eli M. Role of interleukin-8 in tumor growth and metastasis of human melanoma. Pathobiology 1999;67:12–18.
44. Samaniego R, Gutiérrez-González A, Gutiérrez-Seijo A, Sánchez-Gregorio S, García-Giménez J, Mercader E, et al. CCL20 expression by tumor-associated macrophages predicts progression of human primary cutaneous melanoma. Cancer Immunol Res 2018;6:267–75.
45. Acosta JC, O'Loghlen A, Banito A, Guijarro MV, Augert A, Raguz S, et al. Chemokine signaling via the CXCR2 receptor reinforces senescence. Cell 2008;133:1006–18.
46. Lin EC, Amantea CM, Nomanbhoy TK, Weissig H, Ishiyama J, Hu Y, et al. ERK5 kinase activity is dispensable for cellular immune response and proliferation. Proc Natl Acad Sci U S A 2016;113:11865–70.
47. Haferkamp S, Borst A, Adam C, Becker TM, Motschenbacher S, Windhövel S, et al. Vemurafenib induces senescence features in melanoma cells. J Invest Dermatol 2013;133:1601–9.